Kodaikanal Obs. Bull. Ser. A (1980) 3, 36-48

ISODENSITOMETRY OF OMEGA CENTAURI AND 47 TUCANAE

K. K. SCARIA

ABSTRACT

We present details of procedure on equidensitometry of globular clusters using the Sabattier technique in photography. Equidensitometry of Omega Centauri and 47 Tuc shows that both clusters become more elliptical beyond r=2' from the centre when compared to their form close to the centre. Omega Centauri shows a second minimum in ellipticity around 5' from the centre. All clusters for which data on their ellipticity are available exhibit small values close to the centre and a little away from the centre, with a maximum in between. It is suggested that this is the result of peculiarities in the distribution of giant, sub-giant and horizontal branch stars in the cluster. The exact centre of Omega Centauri is given with respect to two bright stars in the field. Multiband equidensitometry of Omega Centauri shows that there is no asymmetric absorption by interstellar dust over the cluster.

Key words : globular clusters—Omega Centauri—47 Tucanae—Multiband equidensitometry—radial change in ellipticity—Sabattier technique

1. Introduction

Many of the globular clusters are elliptical in form. Of the 96 clusters observed by Shapley (1927) for diameter measurements, all except 4, show ellipticities of varying ranges. The largest ellipticity observed for a globular cluster, is for M19 with an axial ratio of about 0.6 (Shapley 1927). The study of ellipticity in globular clusters is important, because of its bearing on the dynamics of these clusters. Pease and Shapley (1917) from star counts show that M13 has an elliptical shape. They also point out that counts of bright stars in Omega Centauri by Bailey show the elliptical nature of the cluster. Star counts of Lindsay (1956) on blue and infrared photographs of Omega Centauri show the cluster to be elliptical even at large distances from the cluster centre. From star counts Dickens and Woolley (1967) find that ellipticity in Omega Centauri is maximum at a distance of about 4' from the centre of the cluster. An application of the star counting technique for determining ellipticity is not possible close to the dense inner regions of globular clusters. Star counts of Lindsay (1956) do not reach closer than 15' from the centre of Omega Centauri. Dickens and Woolley have star counts available for the inner dense regions of Omega Centauri but these are for the brightest stars in the cluster. If we try to reduce overcrowding in the central regions of the cluster by under exposing the photograph, we would only get the distribution of the brightest members, and neglect the fainter ones which actually form the bulk of the mass in the cluster. To study, therefore, the ellipticity in the denser regions we have to use the technique of equidensitometry.

There are many methods available to obtain equal intensity contours on a photographic plate. Some of these procedures are photographic and some are photoelectric. In the photoelectric domain we have the hunting or scanning type of isophotometers. In the photographic field, the Sabattier effect has been usefully exploited to obtain isophotal contours. The merits and demerits of both the methods have been well analysed by Hodge and Brownlee (1966). They point out the simplicity of the photographic method over the photoelectric one.

Detailed accounts of procedure and technique to obtain Sabattiered contours are given by Lau and Krug in their monograph. The astronomical applications of this technique have been studied in detail by Richter and Hogner (1963). They have applied it in their study on the ellipticity of galaxies M31, M32 and NGC 205. Sources of errors and the accuracy of the results have been studied and they have come to

the conclusion that the Sabattier technique is a very sound and reliable method of obtaining isophotes. They find that the attainable minimum distance on Tautenberg Schmidt plates between two isophotes is 0.1 arc minutes on M31, M32, and NGC205. Objects with diameters of about 0.5 arc minutes can be described with good accuracy by 3 or 4 equidensity contours. The effectiveness of the Sabattier technique in many astronomical problems has been demonstrated by Bappu (1978). Sistero and Fourcade (1970) applied Sabattier technique to study ellipticity in Omega Centauri. The 5 equidensity contours they obtained for Omega Centauri show the radial change in ellipticity. Kadla et al. (1976) have used this technique on M3, M5, M13 and M92 to study radial change in ellipticity and orientation of the major axis of the equidensity contours. In the following sections, we show in a detailed way how Sabattier technique is employed on Omega Centauri and 47 Tuc to study radial change in their ellipticity. Similar work is being carried out on other bright globular clusters as well.

2. Details of the Sabattier technique of equidensitometry

Equidensity contours refer to regions of equal transparency or equal blackening on the photographic plate. This is obtained by special copying process using the Sabattier effect. Sabattier effect is the photographic reversal effect which occurs, when one exposes an exposed plate, after a brief development, to a uniform diffuse light once again, and then continues with the full development. In this process, the parts of the plate, which had not been blackened during the first exposure and development, are blackened by the second exposure and subsequent development, whereas the other parts which got developed first, remain unaffected by the second exposure and development. When the second diffuse light exposure is made just sufficient, so that it does not cause total reversal, a certain narrow blackened region of the original plate can be brought out as an equidensity line. In this process, the gamma value of the film used should be high, of the order of 5 to 6. Also a contrast developer should be used. By suitably choosing the gamma value of the plate used, and the proper exposure time while copying, the equidensity lines, can be made to cover any desired density level of the original plate.

The first order equidensity contours are generally broad and cover a large range of density levels. By taking second order and third order equidensity lines, one can go upto the plate limit of the original photograph, which is set by the grain size in it.

3. Sources of Error in Photographic Equidensitometry

For good accuracy in isodensitometry, the source of light in the enlarger unit should be very uniform over the full field of the plate The uniformity of the illumination was checked in our equipment to an accuracy of two per cent and was found to be very uniform. Since, the object of our study is not larger than two or three centimeters in size on the original photographs, the error caused by non-uniform illumination is practically nil. The source of light used for the second exposure is a 25W bulb kept at a distance of two metres from the plate and is covered by opal glass. This keeps the illumination uniform over a large area. The film which was used is "ORWO" F 08 sheet film. It has a high gamma value an is fairly thick.

4. The Determination of equal density contours

The plates that we have used for the equidensitometry of Omega Centauri cover a field of 45 minutes of arc and the densest region of the cluster covers about 20 minutes of arc of this field. We have used the stars in the outer regions of the cluster to match the different contours while making the map. The problem in doing this is that, when we are giving the second exposure, to get the equidensity contour, these stars also will undergo the same process experienced by the cluster and hence in the place of star images, rings will develop. In later stages of processing, these rings will get split further and it may not be possible to use them at all to match the contours. To avoid this difficulty, we have used a mask to cover the field stars and hence while giving the second exposure, the stars outside the cluster, will not get Sabattiered and will remain as black points on a clear background or clear points on a dark background, depending on the stage of equidensitometry. A sample set of equidensity contours is shown in plate II (b). It shows the equidensity contours after three stages of processing. The stars seen are carried through all these stages. Stars T and M of Plate I are also marked in Plate IIb. Since all these stars are available in all sets of equidensity

contours, there is no difficulty in matching the contours. The sets of contours, for map making, are selected in such a way, that the outermost contour in one set matches well with the innermost contour of the next set. Always these overlapping contours match to the finest detail seen in them, which shows the high accuracy of the process. Plate III is a map prepared this way of Omega Centauri. The E-W and N-S directions are marked on the plate.

5. Diffusion of Stellar Images in the Plate

In a globular cluster, the stars are resolved, except in the central regions and hence a direct application of the Sabattier technique will give only a collection of small rings, corresponding to the isophotes of stellar images. The resultant equidensity contours of the cluster are too irregular to measure. Hence, while making the graded exposures of the cluster, for covering regions of different density levels, a thin diffuser is introduced between the film and the original plate (Sistero and Fourcade, 1970). The diffuser increases the size of the stellar image by a factor of about three and hence all the stars get smeared out to give the effect of an out of focus photograph of the cluster. Since, we want only the cluster to be defocussed and the outer star images to be left as they are, we have used a diffuser as shown in plate (II) a. The central circular portion of the plate is the ground portion and the remaining part of the plate is clear glass. The plate also keeps the film pressed well to the holder while taking the graded exposures and avoids any chance of film buckling. In plate II (a), the diffuser is shown against the background of a star field. The details of the central regions of the star field are not lost. Only the images of the stars get defocussed.

6. Reduction of axial ratio and position angle of the isophotes obtained for the cluster

A first attempt at the determination of axial ratio and position angle of the isophotes obtained for a globular cluster, using the Sabattier technique, was made by Kadla (1966) on M13. Sistero and Fourcade (1970) made a similar attempt on Omega Centauri. Kadla (1966) has shown that the ellipticity obtained for M13 by the Sabattier technique, is in good agreement with the results obtained through star counts. Sistero and Fourcade obtained 5 equidensity contours for Omga Centauri and show that the ellipticity decreases towards the centre of the cluster and that the position angle of the major axis changes with distance from the centre. They have checked the results of Sabattier technique, with those obtained through star counts and the results are found to agree satisfactorily. Also they have made extra-focal equidensity curves and checked with the results obtained through the diffuser plate. These are found to be in satisfactory agreement. Hogner et al. (1973) made a detailed study of the dependence of the axial ratio b/a and the position angle ϕ, of the major axis, with distance from the cluster centre, in the globular clusters M3, M5, M13, M15 and M92, in UBV and R bands. In all these clusters the ellipticity reaches a maximum at a certain distance from the cluster centre, which depends on the cluster. Also in some clusters like M92 and M5, the 'b/a' vs 'a' curve shows well defined regions of minimum ellipticity close to the centre and well defined regions of maximum ellipticity at some distance away from the cluster centre. The position angle of the inner region is different from that of the outer region in both these clusters. The differing behaviours of b/a and ϕ in different wavelength bands at distances less than 1' of arc from the centre, are attributed to different distributions of giants and sub-giants.

We have obtained photographs of the cluster Omega Centauri in B, V and the infra-red bands. The details of the photographs are given in Table 1. As explained before, we have obtained isodensity contours in B, V and infra-red bands for the cluster.

Table 1. Details of plate-filter combination used at the 102cm R-C reflector

Kavalur Plate No.	Emulsion	Filter	Scale of Plate	Exposure time	Approx. limiting V Magnitude	Image size of faintest stars
C241	103aO	GG11	40 mm/°	30 min	19.0	20 μ
C25	103aD	C2384	40 mm/°	35 min	17.9	25 μ
5260	1 N	RG9	40 mm/°	90 min	19.5	30 μ

For each contour we have measured x, y coordinates for 72 points on the contour at 5° intervals, along with the x, y coordinates of 2 references stars of the cluster. A computer programme made for the purpose, first translates the arbitrary coordinate system used for measurement, to a new coordinate system such that the origin coincides with the position of one of the reference stars. The new reference system, is then, rotated, so that the x-axis coincides with the direction of the line joining the two reference stars. The coordinates are scaled down taking the distance between the two reference stars as unity. The x, y values are then fitted to a second degree equation of the kind,

$$X^2 + BXY + CY^2 + DX + EY + F = 0$$

by the method of least squares. The solution of the normal equations are done using the matrix inverse method. The properties of the ellipse are derived from the coefficients B, C, D, E and F.

The results have been obtained using two sets of reference stars. Both sets give exactly the same results. The computer programme gives the axial ratio b/a, position angle ϕ, area within each contour, the x and y coordinates of the centre of each contour and the respective errors. The origin for the coordinate system is the star marked T in Plate I and the x-axis is the line joining T and M where M is the second reference star and is marked in Plate I. Since all distances are normalised to the distance TM on every plate, the small difference in the scales of the

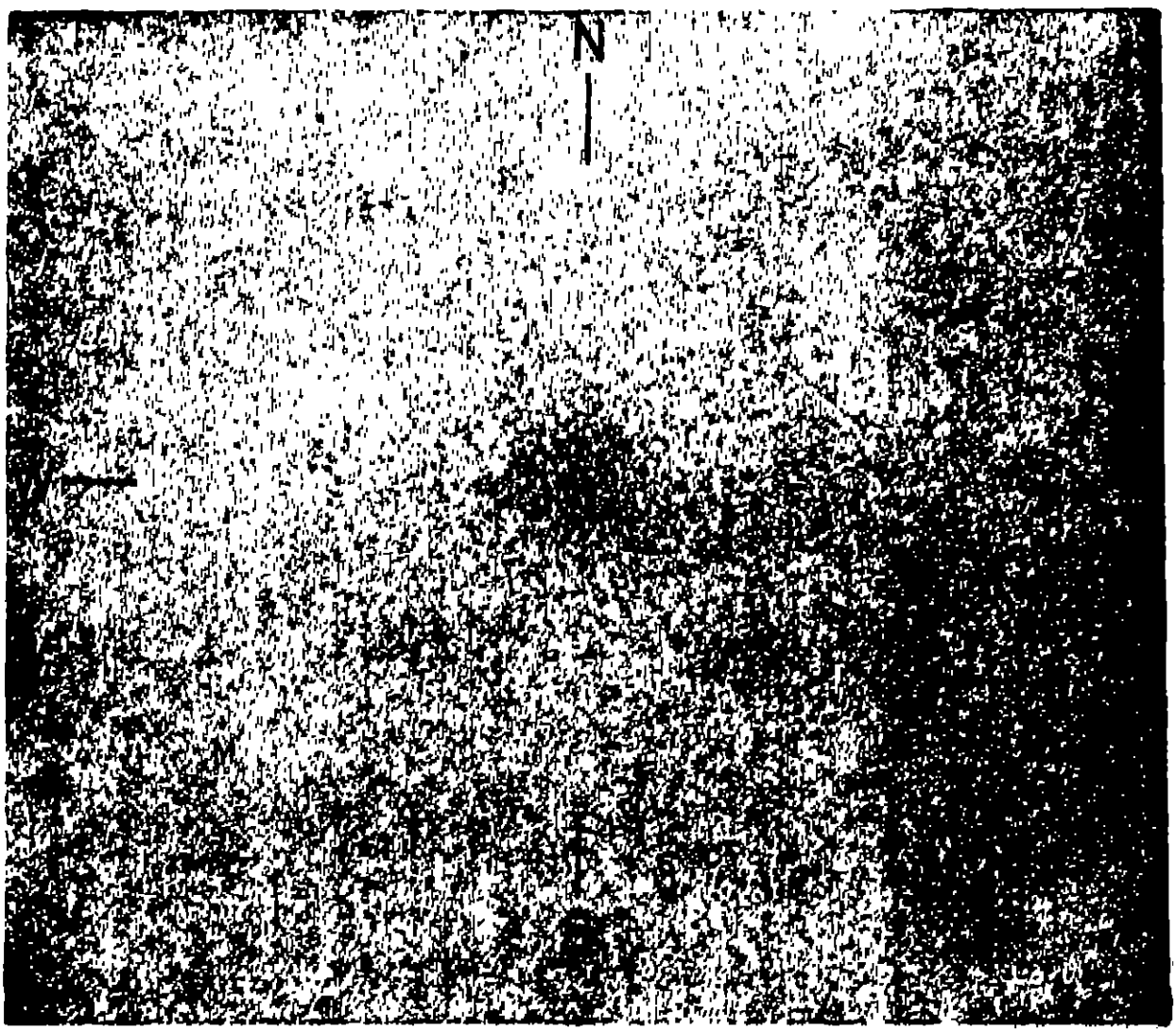

Plate 1. A short exposure photograph of the cluster Omega Centauri in red light. Stars T and M are reference stars. Lines showing NS and EW directions have been marked in such a way that they define the centre of the cluster.

plates taken in B, V and infra-red bands will not cause any error in the results. Knowing the distance of TM – 27.73 arc minutes, all distances can be reduced to arc minutes.

Tables 2 to 4 give the data regarding the equi-density contours obtained for the B, V and infrared bands. Table 2 is for the B band, table 3 is for the V band and table 4 is for the infrared band. In each table, the first column gives the serial number of the contour, the number increasing outward from the cluster centre. Columns 2 and 3 give the semi-major axis (a) and semi-minor axis (b) in arc minutes. Columns 4 and 5 give the x-coordinate of the centre of the cluster with star T as the origin and TM as the x-axis as well as the corresponding error in the least squares fit. Columns 6 and 7 give the y-coordinate of the cluster centre with star T as the origin and TM as the x-axis, and the corresponding error. Column 8 gives the distance between the reference stars in millimetres which gives a check on the scale of the plates used. Since, this distance is taken as unity in the reductions, the plate scale does not come into the picture and small differences in the scale of the photographs taken in B, V and infrared bands will not create any uncertainty in the values derived for each contour and for each band. Columns 9 and 10 give the axial ratio b/a and its error Columns 11 and 12 give the area within each contour in sq. arc min and the corresponding error, while columns 13 and 14 give the position angle of the major axis, ϕ and the corresponding error.

In Figure 1, we have plotted the axial ratio b/a against the semi-major axis 'a' for the B and infrared bands. The values derived for the V band fall between those of the B and infrared bands. These are close to those derived from the B band, because the difference in (B-V) colour is not much from the centre to the edge. Our photometric results (Scarle and Bappu in preparation) show a large difference in (B-I) colour. The curves show that the cluster is definitely less elliptical in the infrared band than it is in the blue band. Both the curves follow the same pattern of increase and decrease in ellipticity with distance from the cluster centre. The curves have three distinct portions. At point H on the curve, ellipticity is the lowest in the cluster. From H to J the ellipticity shows a sharp increase and reaches a maximum at J. Between points J and K, the ellipticity shows a sudden dip. Beyond point K, the

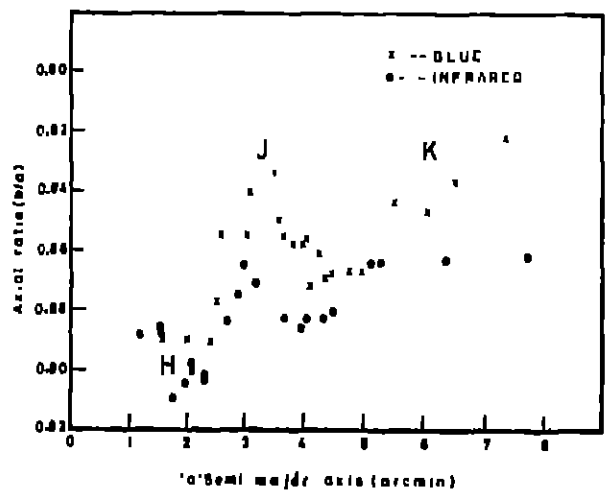

Fig. 1. 'b/a' vs 'a' relation for the cluster Omega Centauri in blue and infrared bands.

ellipticity shows an increasing trend. Point H is at 1.7' from the cluster centre, point J is at 3' and point K is at 5' from the cluster centre. Figure 2 shows ϕ, the position angle plotted against 'a' the semi-major axis. The position angle of the cluster within 1.7' from the centre is definitely different from what the cluster has outside this radius. Beyond 1.7', the position angle shows only slight variations, but these variations, though small, can be connected with the changes in the (b/a-a) curve.

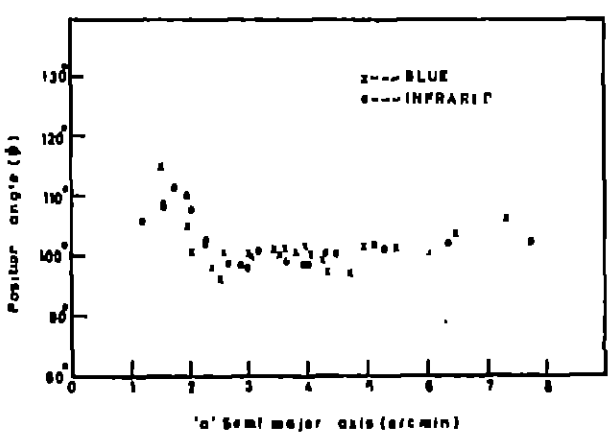

Fig. 2. Position angle 'ϕ' of the major axis of the equidensity contours against semi-major axis 'a'.

7. Isodensitometry of 47 Tuc

47 Tuc is the second largest globular cluster in our galaxy. Basic data on the cluster is taken from Peterson and King (1975) and presented in Table 5.

Table 2. Equidensitometric data for the B plate

Sl. No.	a (arcmin)	b (arcmin)	X_{centre} (arcmin)	σ X_{centre} (arcmin)	Y_{centre} (arcmin)	σ Y_{centre} (arcmin)	Distance TM (mm)	b a	$\sigma_{b/a}$	area (Sq. arcmin)	σ_{area}	ϕ (deg.)	$\sigma\phi$ (deg)
(1)	(2)	(3)	(4)	(5)	(6)	(7)	(8)	(9)	(10)	(11)	(12)	(13)	(14)
1	1.5410	1.3718	15.111	0.005	11.466	0.003	41.9985	0.890	0.006	6.641	0.036	114.5	1.6
2	1.9766	1.7193	15.166	0.003	11 395	0.003	41.9789	0.890	0.004	10.676	0.035	105.1	0.8
3	2 0531	1.8529	15.111	0.005	11.451	0.003	42.0159	0.903	0.005	11.951	0 055	100.8	1 5
4	2.3852	2.1246	15.194	0.005	11.423	0.003	41.9704	0.891	0.004	15.920	0 056	98.0	1.0
5	2.5108	2.2028	15.111	0 005	11.461	0.003	41.9985	0 877	0.003	17.375	0.052	96 2	0.7
6	2.6012	2.2231	15.194	0.005	11.368	0.005	41.9789	0.855	0.004	18.167	0.061	100.7	0.7
7	3.0422	2.6005	15.109	0.008	11.403	0.006	42.0018	0.855	0.005	24.853	0.099	100.5	0 8
8	3.0945	2.6010	15.111	0.008	11.423	0.005	41.9474	0.841	0.005	25.286	0.096	100.4	0.7
9	3.4560	2.8810	15.111	0.008	11.423	0.005	41.9630	0.834	0.005	31.280	0 130	101.3	0.7
10	3.5602	3.0249	15.055	0.008	11.395	0.005	41.9845	0.850	0.005	33.832	0.140	100.3	0.8
11	3.6501	3.1196	15.109	0.010	11 403	0.008	42.0018	0.856	0.005	35.772	0.157	101.3	0.9
12	3.8147	3 2742	15.109	0.010	11.403	0.008	42.0018	0.858	0.005	39 238	0.164	100.5	0.9
13	3.9834	3.4163	15.111	0.010	11.423	0.008	41.9630	0.858	0.005	42.752	0.199	101.8	1.0
14	4.0294	3.4483	15.109	0.012	11.403	0.010	42.0018	0.856	0.005	43.651	0.202	99.5	1.0
15	4.0815	3.5572	15.055	0.011	11.451	0.008	42.0166	0.872	0 005	45.611	0.190	100.4	1.0
16	4.2729	3.6801	15.109	0.010	11.403	0.008	42.0018	0.861	0.005	49 400	0.193	99.6	0.8
17	4.3610	3.7898	15.083	0.008	11.423	0 008	41 9845	0.869	0.004	51.922	0.175	97.1	0.8
18	4.4727	3.8838	15.055	0.008	11.423	0.005	42.0092	0.868	0 003	54 572	0.175	100.2	0 7
19	4.7511	4.1170	15.083	0.008	11.395	0.008	41.9845	0.867	0.004	61.450	0 234	97.4	0.9
20	4.9551	4.2969	15 027	0.008	11.423	0 008	42.0159	0.867	0.004	66.889	0.250	101 8	0 8
21	5 4877	4.6324	15.166	0.012	11.285	0.008	42.0092	0.844	0.005	79.863	0.383	101.4	0.9
22	6.0401	5.1185	15.027	0.012	11.423	0 013	42.0159	0.847	0 005	97.088	0.449	100.6	0.9
23	6.4897	5.4328	15.111	0.016	11.229	0.013	42.0092	0.837	0.005	110 763	0.522	103.8	0.9
24	7.3260	6.0212	15.194	0.020	11.395	0 018	42.0159	0.822	0.006	138.579	0.669	106.1	0.8

Table 3. Equidensitometric data for the V plate

Sl. No.	a (arcmin)	b (arcmin)	X_{centre} (arcmin)	$\sigma_{X_{centre}}$ (arcmin)	Y_{centre} (arcmin)	$\sigma_{Y_{centre}}$ (arcmin)	Distance TM (mm)	b/a	$\sigma_{b/a}$	area (arcmin)	σ_{area} (arcmin)	ϕ (deg.)	σ_ϕ (deg.)
(1)	(2)	(3)	(4)	(5)	(6)	(7)	(8)	(9)	(10)	(11)	(12)	(13)	(14)
1	0.8164	0.7461	15.129	0.005	11.575	0.005	41.3405	0.915	0.016	1.911	0.029	102.3	5.1
2	1.1368	1.0397	15.096	0.003	11.614	0.003	41.3652	0.915	0.007	3.713	0.022	109.6	2.1
3	1.3128	1.1967	15.063	0.003	11.647	0.003	41.3009	0.912	0.006	4.935	0.025	125.9	1.8
4	1.3879	1.2485	15.110	0.005	11.647	0.003	41.2916	0.900	0.006	5.443	0.029	128.3	1.7
5	1.7553	1.5577	15.110	0.003	11.619	0.003	41.3470	0.887	0.004	8.589	0.033	112.4	1.0
6	1.8241	1.6167	15.110	0.003	11 619	0.003	41.3652	0.886	0.004	9.264	0.029	111.1	0.9
7	2.4141	2.1210	15.074	0.005	11.589	0.005	41.3652	0.879	0.004	16.085	0.061	101.5	1.0
8	2.4474	2.1506	15.077	0.005	11.592	0.005	41.3470	0.879	0.004	16.535	0.068	98.1	1.1
9	2.5976	2.3018	15.138	0.008	11.567	0.008	41.3092	0.886	0.007	18.784	0.113	104.1	1.7
10	2.6902	2.3780	15.165	0.008	11.562	0.005	41.3303	0.884	0.005	20.097	0.089	98.1	1.2
11	2.7099	2.3528	15.116	0.005	11.586	0.005	41 3652	0.868	0.005	20.030	0.084	98.6	0.9
12	2.7870	2.4135	15.105	0.008	11.575	0.005	41.3470	0.866	0.005	21.131	0.092	98.4	1.0
13	2.9597	2.5771	15.138	0.008	11.562	0.005	41.3092	0.871	0.005	23.962	0.125	101.7	1.3
14	3.2070	2.7102	15.105	0.008	11.553	0.005	41.3253	0.845	0.004	27.305	0.101	98.9	0.7
15	3.5436	3.0207	15.060	0.008	11.553	0.008	41.2945	0.852	0.005	33.628	0.139	99.4	0.9
16	3.7651	3.2549	15.082	0.008	11.589	0.008	41.2852	0.865	0.005	38.500	0.168	98.0	1.0
17	3.8821	3.3764	15 077	0.012	11.581	0.008	41.3252	0.870	0.005	41.178	0 192	100.1	1.1
18	4.2068	3.6088	15.043	0.012	11.581	0 008	41.3045	0.858	0.005	47.694	0.199	98.8	0.9
19	4.4655	3.8489	15.013	0.012	11.594	0.008	41.3352	0.862	0.005	53 995	0.224	97.6	0.9
20	4.9410	4.3174	15.004	0.016	11.594	0.014	41.3352	0.874	0.007	67.017	0.404	98 9	1.4
21	5.2684	4.4439	15.030	0.018	11.558	0.016	41.3252	0.844	0.007	73.551	0.461	96.0	1.2
22	5.8892	4.9413	14.944	0.018	11.506	0.016	41.3045	0.839	0.007	91.421	0.527	99.1	1.1
23	6.0606	5.1013	15.069	0.020	11.568	0.016	41 3252	0.842	0.008	97.128	0.617	93.3	1.2
24	7.4221	6.1504	14.694	0.027	11.200	0.021	41.3045	0.829	0.008	143.410	0.896	98.5	1.1

Table 4. Equidensitometric data for the Infrared plate

Sl. No.	a (arcmin)	b (arcmin)	X_{centre} (arcmin)	$\sigma_{X_{centre}}$ (arcmin)	Y_{centre} (arcmin)	$\sigma_{Y_{centre}}$ (arcmin)	Distance TM (mm)	b/a	$\sigma_{b/a}$	area (Sq. arcmin)	σ_{area}	ϕ (deg.)	σ_{ϕ} (deg)
(1)	(2)	(3)	(4)	(5)	(6)	(7)	(8)	(9)	(10)	(11)	(12)	(13)	(14)
1	1.1889	1.0564	15.165	0.008	11.256	0.008	42.7798	0.888	0.013	3.945	0 045	105.9	3.3
2	1.5313	1.3580	15.165	0.005	11.311	0.005	42.7808	0.886	0.006	6.523	0.036	108.2	1.5
3	1.5477	1.3760	15.138	0.005	11.339	0.005	42.7714	0.889	0.007	6.690	0.040	108.7	1.7
4	1.7492	1.5920	15.138	0.005	11.339	0.005	42.7606	0.910	0.007	8.748	0 055	111.4	2.2
5	1.9486	1.7634	15.138	0 005	11.339	0.005	42.7844	0.905	0.005	10.795	0.051	110.0	1.6
6	2.0340	1.8269	15.165	0.005	11.339	0.005	42 7613	0.898	0.005	11.673	0.051	107.9	1.4
7	2.2834	2.0625	15.138	0.005	11.311	0.005	42.7736	0.904	0.005	14.795	0.063	102.0	1.4
8	2.2956	2.0702	15.138	0.005	11.339	0.005	42 7767	0.902	0.004	14.930	0.054	102.6	1.2
9	2.6852	2.3728	15.165	0.005	11.311	0.005	42.7844	0.884	0.004	20.016	0.073	99 0	1.0
10	2.8982	2.5358	15.138	0.008	11.339	0.005	42.7955	0.875	0.004	23.088	0.095	98.7	1.0
11	3.0066	2,6007	15 193	0.008	11.284	0.005	42.7844	0.865	0.004	24.564	0.099	98.2	0.9
12	3.1868	2.7759	15.221	0.008	11.339	0 005	42.7901	0.871	0.005	27.791	0.124	100.9	1.1
13	3.6605	3.2298	15.165	0.011	11.450	0.008	42.7973	0.883	0.005	37.142	0.183	99.0	1.3
14	3.9386	3.4884	15.110	0.011	11.367	0.008	42.7955	0.886	0.005	43.163	0.195	98.7	1.2
15	4.0298	3.5678	15.138	0.008	11.395	0.008	42.7968	0.883	0.004	45.041	0.168	93.4	1.0
16	4.3418	3.8339	15.193	0.008	11.339	0 005	42.7901	0.883	0.003	2.2	0.161	100.5	0.8
17	4.4918	3.9587	15.165	0.008	11.450	0.005	42 7973	0.881	0.003	55.862	9.163	100.2	0.8
18	5.1069	4.4134	15.055	0.011	11.367	0.008	42.7968	0.864	0.005	70.807	0.319	102.0	1.0
19	5.2911	4.5706	15.055	0.016	11.367	0.010	42.7585	0.864	0.006	75.974	0.420	101.1	1.2
20	6.3795	5.5044	15.135	0 018	11.311	0.012	42.7644	0 863	0.006	110.318	0.573	102.0	1.2
21	7.7530	6.6852	14.944	0.024	10.951	0.014	42.7587	0.862	0.006	162.829	0.837	102.2	1.1

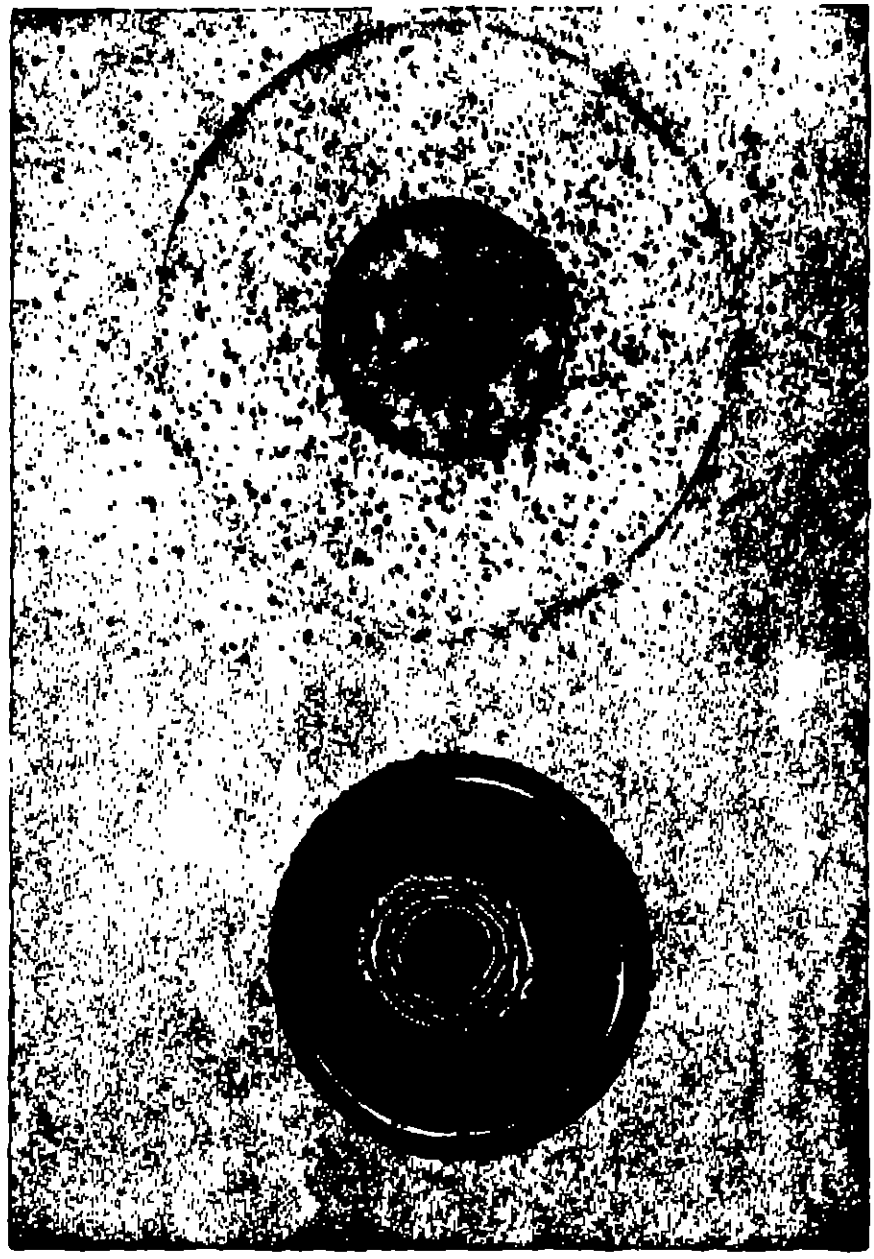

Plate 2a, b. 2(a) shows the diffuser plate against a star field. Since only the central part of the glass piece is ground, the stars in this region alone get defocussed and other stars remain in focus. 2 (b) shows a sample set of contours after three stages of Sabattier processing. Reference stars T and M are marked.

When compared to Omega Centauri, this is a cluster that is more centrally concentrated and is one that is also closer to us. The metallicity of the cluster is larger than that for Omega Centauri. Compared to the large core-radius of Omega Centauri (≈2.5'), 47 Tuc has a small core-radius $r_c = 0',41$ (Peterson and King 1975). Gascoigne and Burr (1956) have made drift scan and concentric aperture measures on the cluster in P and V bands. They show a radial colour change of 0.17 in P-V colour. Chun and Freeman (1979) have studied the cluster photoelectrically, making spot measurements on 81 locations on the cluster in U, B, V bands. Photoelectric measurements of the Mg b lines and the blue CN band were also made on these locations. They report a colour change in the cluster at a distance of about 2' from the centre. The results for the CN bands were not conclusive and the Mg b lines did not

Table 5

1950	1950	(° deg)	(b° deg)	Conc. Class	Sp. Type	Vr kms/sec	$(m-M)_{app.\ V}$
$00^h\ 21.8^m$	−72° 21′	306	−45	III	G3	−24	13.15

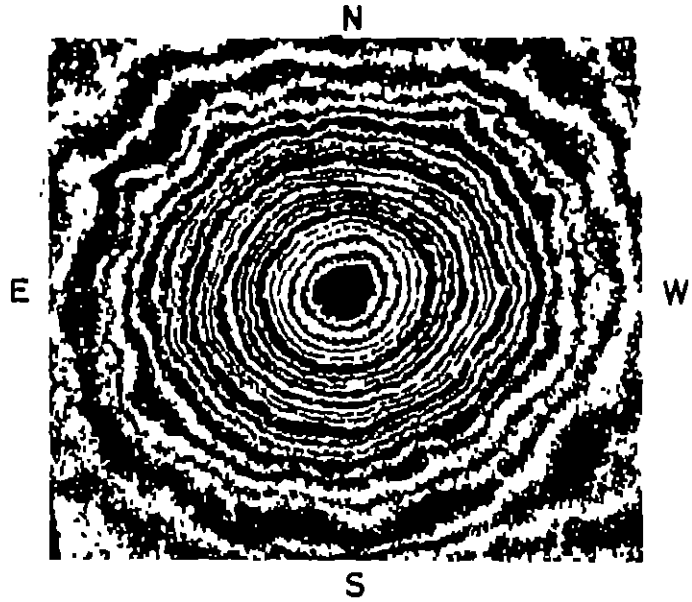

Plate 3. Equidensity contours for the cluster Omega Centauri.

show any obvious variation. The core-radius of the cluster is only 0′.41. Hence, the 59″.4 diaphragm used by Chun and Freeman for the spot measurements is too large to show the exact location of the colour change in the core. The B-V colour of the inner region of radius 2′ is −0.90 mag and the U-B colour is −0.39 mag. Outside this region the colour decreases to B-V −0.81 mag and U-B −0.25 mag at radius 4′.

The plates we have used for equidensitometry of 47 Tuc were taken by the 60 inch reflector at the Bloemfontein Station of Harvard Observatory. The scale of the plate is 26″/mm. The details regarding the plate are given in Table 6.

The procedure followed for obtaining the isophotes was the same as before. 18 contours have been obtained for the cluster. Following the same procedure as before, the axial ratio, the semi major and semi minor axes and the position angle were determined. The first column in Table 7 gives the contour number, the number increasing outward in the cluster. Column 2 gives 'a' the semi major axis. Column 3 and 4 give b/a, the axial ratio and its errors. Column 5 gives the position angle ϕ. In Figure 5 we have plotted b/a and ϕ against the semi major axis 'a'. The change in ellipticity in the cluster is similar to what is seen in Omega Centauri. The minimum seen beyond the point of maximum ellipticity is not so prominent as it is in the case of

Table 6

Plate No.	Date	Station	Telescope	Exposure Time	Scale of the Plate
SB 192	Sept. 19/11 1934	Bloemfontein	60″ Reflector	180 minutes	26″/mm
SB 2077	Nov. 9/10 1939	,,	,,	1 minute	,,

Omega Centauri. The region of smallest ellipticity in the cluster extends upto r = 1.20 arc min from the centre. The ellipticity increases, thereafter, and reaches a peak around 2.4' from the centre. The ellipticity shows a small decrease between 2.4' and 4' and beyond this, the ellipticity is found to increase considerably as seen in the figure. But the results obtained for this region of the cluster are not conclusive, as the plate used for the purpose was not exposed sufficiently for recording the faint outer region of the cluster. Hence, the uncertainties in these outer portions can be quite large. The change in the position angle does not show the kind of change seen in the other three clusters. The position angle changes in a way similar to the change in ellipticity.

Table 7
Equidensitometry of 47 Tuc

Sl. No.	'a' in minutes of arc	b/a axial ratio	σ b/a	φ degree
1	0.67	0.974	0 001	14.4
2	0.74	0.969	0.002	34.7
3	0.79	0.972	0.002	54.7
4	1.15	0.971	0.003	71.4
5	1.32	0.967	0.003	49.4
6	1.56	0.929	0.004	49.3
7	1.76	0.930	0.004	46.9
8	2.09	0.914	0.005	60.6
9	2.38	0.907	0.005	63 2
10	2.64	0.909	0.005	62.6
11	2.93	0.917	0.006	59.9
12	3.24	0.920	0.006	61.5
13	3.59	0.915	0.007	45.1
14	4.05	0.913	0.008	40.3
15	4.68	0.917	0.008	51.5
16	6.06	0.923	0.009	53.5
17	7.00	0.797	0.010	51.3
18	7.79	0.863	0·015	58.3

8. Results of equidensitometry on Omega Centauri and 47 Tuc

In Fig. 3, we have plotted the x and y, coordinates of the centres of each contour against their semi-major axis 'a' expressed in arc minutes. The centres of blue equidensity contours are marked by crosses and the centres of infrared equidensity contours are marked by filled circles. The close agreement between the centres of blue and infrared equidensity contours show that there is no asymmetrical absorption over the cluster due to the presence of dust. Table 8 gives the mean values of the x and y coordinates of the centre of the cluster for the 3 wavelength bands B, V and infrared. From the table, we can find the location of the exact centre of the cluster with respect to the two reference stars T and M. This centre is marked in plate 1 which when compared with the centre of the cluster determined by Martin (1938) from star counts of bright stars is found to be off by ≈2 seconds of arc.

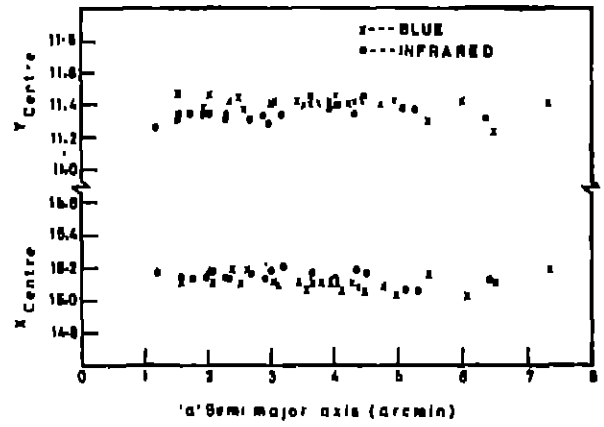

Fig. 3. x and y coordinates of the centres of the equidensity contours obtained from the blue and infrared photographs of the cluster Omega Centauri, with star T as the origin and TM as the x-axis, are plotted against 'a' the semi-major axis.

Table 8

Wave length band	X centre in arc minutes	Y centre in arc minutes
B	15.109	11.403
V	15.085	11.568
Infrared	15.136	11.327
Mean	15.103	11.423

Fig. 4 shows a plot of the axial ratio b/a against 'a' the semi major axis, for the clusters M92 and Omega Centauri, in the B band. Data for M92 is taken from Hogner et al (1973). Taking the distance of Omega Centauri and M92 as 5.4 kpc and 8.1 kpc (Peterson and King 1975) respectively from the sun, the major axis values of M92 have been normalised to the scale of Omega Centauri. Ellipticity curves for M92 and Omega Centauri are similar in every respect. The position angle of the major axis of the equidensity contours of M92 show changes similar to

what is seen in the case of Omega Centauri. In both cases the position angle close to the centre is much different from the position angle for the outer regions. These show that whatever dynamical situation prevails in Omega Centauri, also does in M92. In Fig. 5 we find sudden increase in ellipticity in the case of 47 Tuc, beyond 1'.4 from the centre. Kadla et al (1976) show radial change in ellipticity in clusters M3, M5, M13 and M15. The 'b/a' vs 'a' and 'ϕ' vs 'a' plots for M5 behave exactly like those for M92 and Omega Centauri Similar plots for M3, M13 and M15 also show the sudden increase as well as the second minimum in ellipticity very clearly.

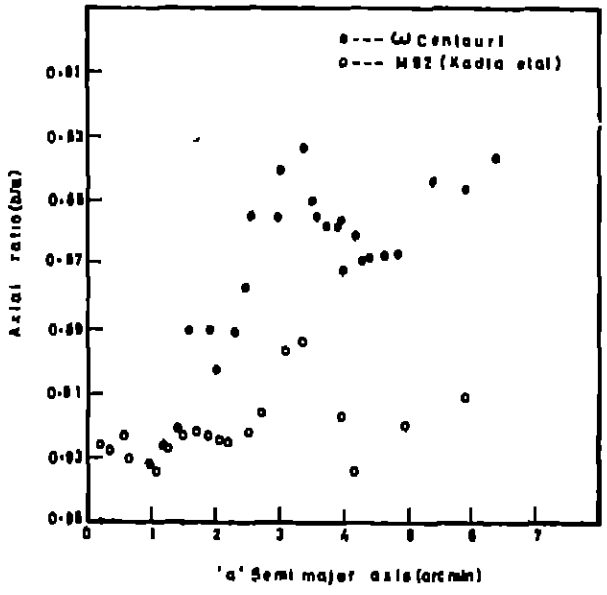

Fig. 4. 'b/a' vs 'a' relation for Omega Centauri and M92. Data for M92 are taken from Hegner et al (1973). The values of ordinate for M92 have been normalised to the distance of Omega Centauri.

We also find from Fig. 1 that the cluster is more spherical in infrared light than in the blue light. The increase in ellipticity is more noticeable in the blue band. This probably suggests that the observed changes in ellipticity could be the result of peculiarities in the distribution of giant, sub-giant and blue horizontal branch stars in the cluster.

Harding (1956) gives evidence for rotation in Omega Centauri. Dickens and Woolley 1967 find that the flattening observed in Omega Centauri can be explained by the observed rotation of the cluster. King (1980) points out that ellipticity in the inner parts of dense globular clusters, where the relaxation time is much smaller when compared to the age of the cluster,

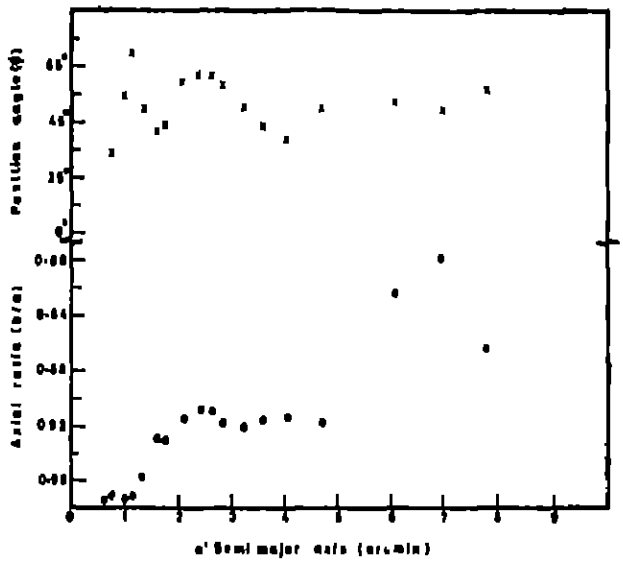

Fig. 5. 'b/a' vs a' and 'ϕ' vs 'a' relations for 47 Tuc. Increase in ellipticity beyond 1'.5 from the cluster centre is clearly seen.

must be due to rotation. Hence, radial change in ellipticity in globular clusters may be indicative of radial differences in rotational velocities in the cluster. Hence, it is important to see whether there is any radial change in velocity dispersion in globular clusters and look for a peak in the intermediate region where the ellipticity is found to increase.

Scaria and Bappu (unpublished) find that Omega Centauri is bluer between 2' and 4' from the centre with respect to the colour at the centre. This is the region where ellipticity in Omega Centauri increases considerably. The same relation is found to hold in the case of 47 Tuc. Gascoigne and Burr (1956) and Chun and Freeman (1979) find that 47 Tuc is bluer between 2' and 4' from the cluster centre. Our results on ellipticity of 47 Tuc show that the cluster is more elliptical in this region. Thus, a relationship seems to be apparent between the increase in ellipticity and change in the colour of the cluster as noticed in several globular clusters. For a thorough understanding of the problem, we need many more observations of this kind.

Acknowledgements

I am indebted to Prof. M.K.V. Bappu for suggesting this project and for advice and guidance during the course of the study. I am also grateful to Mr. A. V. Raveendran for giving me much assistance in the processing of the data. I am thankful to Prof. W. Liller of Harward Observatory for lending me the photographs of 47 Tuc for equidensitometry.

References

Bappu, M.K.V. 1978, Proc. ESO workshop on Modern Techniques in *Astronomical photography*, Eds. R. M. West and J.L. Heudier, ESO, Geneva, p. 263.

Chun, M.S., Freeman, K.C. 1979, *Astrophys. J.* 227, 93.

Dickens, R.J., Woolley, R. Vd. R. 1967, *R. Obs. Bull.* No. 128.

Gascoigne, S. C. B. Burr, E. J. 1956, *Mon. Not. R. astr. Soc.*, 116, 570.

Harding, G.A. 1965, *R. Obs. Bull.*, No. 99.

Hodge, P.W., Brownlee, D.E. 1966, *Publ. astr. Soc. Pacific*, 78, 125.

Hogner, W., Kadla, Z.I., Richter, N., Strugatskaya, A.A. 1973, Soviet *Astr.*, 16, 843.

Kadla, Z.I. 1966, Soviet *Astr.*, 10, 97.

Kadla, Z.I., Richter, N., Strugatskaya, A.A., Hogner, W. 1976 *Soviet Astr.*, 20, 49.

King, I.R. 1980, in Globular Clusters Eds D. Hanes and B. Madore, Cambridge University Press, p. 249.

Lindsay, E. M. 1956, In Vistas in Astronomy, Ed. A. Beer, Pergamon Press, New York, p. 1057.

Martin, W. Chr. 1938, Ann Sterrew. Leiden, XVII, Part 2.

Pease, F.G., Shapley, H. 1917, *Mt. Wilson Observatory Communication* No. 38.

Peterson, C.J., King, I.R. 1975, *Astr. J.*, 80, 427.

Richter, N., Hogner, W. 1963, *Astr. Nachr.* 287, 261.

Shapley, H. 1927, *Harvard College Observatory Bull.* No. 852.

Sistero, R.F., Fourcade, C.R. 1970, *Astr. J.*, 75, 34.